

Robert Knuteson\*, Fred Best, Ralph Dedecker, Ray Garcia, Sanjay Limaye, Erik Olson, Henry Revercomb, and David Tobin

Space Science and Engineering Center, University of Wisconsin-Madison

The Geosynchronous Imaging Fourier Transform Spectrometer (GIFTS) instrument, under development for the NASA New Millennium Program, will serve as a valuable test bed for the evaluation of approaches to flight hardware and ground data processing in the years leading up to NOAA's operational Hyperspectral Environmental Suite (HES). The GIFTS sensor makes use of a 2-D array of detectors to increase area coverage rates while providing dramatically higher vertical resolution by measuring the thermal infrared upwelling emission spectrum at high spectral resolution. The sensor calibration makes use of two internal high precision blackbody references in addition to an external view to space. The GIFTS ground data processing algorithms used to convert from instrument values (Level 0 data) to geo-located, calibrated radiances (Level 1 data) are under development at the University of Wisconsin Cooperative Institute for Meteorological Satellite Studies (UW-CIMSS). These algorithms include geo-location, non-linearity correction, calibration, and correction for off-axis effects. This paper provides a description of the Level 0-1 GIFTS algorithms and their performance characteristics.

## 1. INTRODUCTION

The U.S. National Oceanic and Atmospheric Administration (NOAA) operates geostationary operational environmental satellites (GOES) for short-range warning and nowcasting, and polar-orbiting environmental satellites (POES) for longer term forecasting. GOES satellites provide continuous monitoring from space in a geosynchronous orbit about 35,800 km (22,300 miles) above the Earth. The current generation of GOES satellites contain separate imager and sounder instruments. The sounder is used to remotely sense the atmospheric thermodynamic state, e.g. atmospheric stability and total column water vapor. A new generation of sensors are under development that will greatly increase the horizontal, vertical, and temporal sampling of the GOES sounder and provide a truly four-dimensional view of the Earth's atmosphere. NOAA's plan for a Hyperspectral Environmental Suite (HES) calls for the replacement of the current GOES instrumentation starting as early as 2013 (Dittberner et al. 2003; Gurka et al. 2003). Meanwhile, NASA's New Millennium Program Earth Observing 3 (NMP EO3) mission is the first step in improving the U.S. geostationary weather observing system. The NMP EO3 mission features the Geosynchronous Imaging Fourier Transform Spectrometer (GIFTS), an instrument that incorporates new technologies to implement an innovative atmospheric measuring concept proposed by Dr. William L. Smith of NASA's Langley Research

Center (Smith et al. 2000). The NASA GIFTS research instrument will serve as a valuable test bed for the evaluation of approaches to flight hardware and ground data processing in the years preceding the implementation of NOAA's operational Hyperspectral Environmental Suite.

This paper provides an overview of the algorithm theoretical basis document (ATBD) that is being written by the University of Wisconsin Cooperative Institute for Meteorological Satellite Studies (UW-CIMSS) describing the science algorithms required in the ground processing of GIFTS data. The scope of this document is limited to the algorithms needed for the conversion of raw instrument counts (Level 0 data) to calibrated radiances (Level 1 data). The geo-location approach is described in Limaye et al. (2004) while the science algorithms for higher level products (2+) are described in Huang et al. (2004).

## 2. INSTRUMENT DESCRIPTION

The GIFTS instrument is an imaging Fourier Transform Spectrometer (FTS) designed to provide significant advances in water vapor, wind, temperature, and trace gas profiling from geostationary orbit. Imaging FTS offers an instrument approach that can satisfy the demanding radiometric and spectral accuracy requirements for remote sensing and climate applications, while providing the massively parallel spatial sampling needed for rapid high spatial resolution coverage of the Earth disk, as well as more frequent coverage of selected regions. The GIFTS baseline design uses focal plane detector arrays to cover two

\* *Corresponding author address:* Robert Knuteson, 1225 W. Dayton St., University of Wisconsin-Madison, Madison, WI 53706; [robert.knuteson@ssec.wisc.edu](mailto:robert.knuteson@ssec.wisc.edu)

broad spectral regions; a longwave infrared band (685–1129  $\text{cm}^{-1}$ ) and a midwave/shortwave band (1650–2250  $\text{cm}^{-1}$ ). Each focal plane array contains a grid of 128 x 128 elements for a total of 16,384 fields of view with a nominal field of view diameter of 4 km at the sub-satellite point. Details of the initial instrument design are described in Bingham et al. (2000).

### 3. ALGORITHM DESCRIPTIONS

The GIFTS sensor will sample the interferogram from each detector as a function of optical path delay and numerically filter the data in real-time to reduce the data rate before transmission to the ground-based X-band receiver. The sensor will obtain views of the onboard calibration references and deep space at regular intervals interleaved with the observations of Earth scenes. The ground reception facility will decode the telemetry stream and pass the GIFTS sensor data in real-time to a ground data processing facility. The GIFTS Level 0 to 1 ground data processing is anticipated to include the following tasks: i) Fourier transform of the GIFTS interferograms, ii) application of a non-linearity correction to the sensor data, iii) radiometric calibration, iv) spectral calibration, v) instrument line shape correction, and vi) spectral resampling to a common wavenumber grid.

#### 3.1 Fourier Transform

One of the first operators applied to the GIFTS sensor data will be a Fourier transform to convert the measured interferograms into complex spectra. Since the measured interferograms (real) have been numerically filtered and decimated on-board using a complex function, the Level 0 interferograms are a series of complex numbers as a function of point number. A complex Fourier transform and data folding will be performed to convert the complex interferograms to complex spectra corresponding to a wavenumber scale that will be assigned in the spectral calibration process. There are a number of fast Fourier transform algorithms that could be used for this operation and the actual choice of FFT algorithm is deferred to the implementation stage. It is important to note, however, that the same FFT algorithm must be used throughout the Level 0 to 1 processing to avoid numerical inconsistencies. One of the implementation decisions will be whether to “zero fill” or truncate the measured interferograms to a convenient number of points to optimize computational efficiency.

#### 3.2 Non-linearity Correction

The precise treatment of non-linearity is pending the collection of GIFTS ground test data using flight detectors. The expectation is that the GIFTS detector material should be highly linear in the range of photon fluxes used, but the electronics readout of the focal plane array can introduce a small signal non-linearity.

The non-linearity correction algorithm to be used for the GIFTS interferometric data is based on the successful application of this technique to MCT detectors on the UW-CIMSS ground-based AERI instrument and the UW-CIMSS Scanning-HIS instrument (Revercomb et al. 1998). The signal coming out of the detector readout is composed of an interferogram plus a scene dependent DC offset. The quadratic non-linearity can be modeled as the true signal plus an additional term made up of an unknown coefficient times the square of the sum of the true signal plus the DC level. In the spectral domain, this quadratic non-linearity has two terms; the first is slowly varying in wavenumber with a peak near zero wavenumber while the second term is linear in the uncalibrated spectrum. This non-linearity signature is quite different from that of conventional radiometers and means that the non-linearity coefficients can be determined independently from other calibration errors. The application of a non-linearity correction involves the reconstruction of the readout signal from the numerically filtered interferogram and the application of the quadratic correction. Higher order corrections can be applied if needed.

#### 3.3 Radiometric Calibration

The top-level GIFTS calibration requirement is to measure brightness temperature to better than 1 K, with a reproducibility of  $\pm 0.2$  K. A calibration concept has been developed for the GIFTS instrument configuration (Best et al. 2000). For in-flight radiometric calibration, GIFTS uses views of two on-board blackbody sources (300 K and 265 K) along with cold space sequenced at regular, programmable intervals. The temperature difference between the two internal blackbody views provides the sensor slope term in the calibration equation, while the deep space view corrects for radiant emission from the telescope by establishing the offset term. The blackbody references are cavities that follow the University of Wisconsin (UW) Atmospheric Emitted Radiance Interferometer (AERI) design, scaled to the GIFTS beam size (Best et al. 1997).

Two options were considered for the GIFTS radiometric calibration implementation. One follows the traditional approach of using a large area external blackbody viewed with a flat pointing mirror that is also used to view cold space and the earth (e.g., the current GOES imager and sounder). The second option replaces the large area external blackbody with a pair of internal small cavity blackbodies at different temperatures. Here we mainly discuss the internal blackbody approach, but the overall performance of both systems is compared and shown to meet advanced sounding requirements.

Assume that we represent the complex, uncalibrated spectrum for incident radiance  $N$  by

$$C = [N\tau_i + B_i(1 - \tau_i)]R_f + C_f \quad (1)$$

where  $\tau_t$  is the transmission of the telescope (and external pointing mirror, if included),  $B_t$  is the Planck emission at the temperature of the telescope,  $R_f$  is the complex responsivity of the portion of the instrument behind the telescope, and  $C_f$  is the complex offset arising from the same portion of the instrument behind the telescope. The term in the square brackets is the radiance incident on the turning flat, assuming there is no scattering from the telescope mirror. Similarly, the uncalibrated spectra for the internal hot and cold blackbodies can be represented as

$$C_H = B_H R_f + C_f \text{ and } C_C = B_C R_f + C_f \quad (2)$$

where the radiance emitted by the blackbodies is represented by  $B_H$  and  $B_C$ . Differencing the equations in (2) shows that the complex responsivity is given by

$$R_f = \frac{C_H - C_C}{B_H - B_C} \quad (3)$$

Therefore, the responsivity excluding the telescope can be monitored without changing the instrument pointing. Careful control of the detector temperature and use of low temperature-coefficient electronics should make the responsivity a very stable quantity.

Now, since the space view raw spectrum is given by Equation 1 with the scene radiance  $N$  replaced by  $B_s$  (which consists of space emission and any warmer tail of the field of view), differencing an earth view  $C_E$  at time  $t_E$  and a space view  $C_S$  spectrum interpolated to time  $t_E$  yields the relationship

$$N = \frac{1}{\tau_t} \text{Re} \left( \frac{C_E - C_S}{R_f} \right) + B_s = \frac{1}{\tau_t} (B_H - B_C) \text{Re} \left( \frac{C_E - C_S}{C_H - C_C} \right) + B_s \quad (4)$$

where Equation 3 has been used to eliminate the complex responsivity and where  $\text{Re}$  stands for the real part of the complex spectral ratio. The subtraction of the background assumes that instrument emissions have not changed significantly between the space view and the earth view. In practice, the space views must be performed frequently enough that temporal interpolation can approximate the required simultaneity with only small errors. When the telescope transmission is known, Equation 4 is the basic calibration relationship. In fact, the transmission will be measured both from piece-part reflectivity measurements and from full aperture blackbody observations on the ground, so it will be well known at the start of the mission. The equation is very similar to that for a full aperture "hot" blackbody calibration approach for which the cold blackbody raw spectrum in the denominator would be replaced by the space view spectrum  $C_S$ . The telescope transmission can also be determined in flight using internal blackbody and space views as described in Best et al. (2000). Note that in Equation 4, the ratio of differences of complex

spectra automatically eliminates the phase of the raw spectra (Revercomb et al. 1988). As for an external blackbody calibration, phase correction is not needed and in fact, should be avoided. The details of algorithm implementation are deferred to a future paper.

Figures 1 and 2 show the GIFTS baseline calibration radiometric accuracy compared to the external blackbody approach, assuming the same parameter uncertainties for both, except for the emissivity uncertainty of the external blackbody (increased to 0.005 to account for its lower cavity enhancement factor). At each scene temperature, the calibration accuracy is the root sum square (RSS) combination of several system uncertainties, including those due to temperature and emissivity for each of the blackbodies, the structure temperatures affecting reflection from the blackbodies, and the telescope mirror reflectivity. Also included is the contribution from the time variation of the telescope temperature between the space and earth views. For the case where the transmission is known, we have assumed that ground based testing with a large external blackbody has determined the transmission of the telescope to within 0.2%. Table 1 presents the input parameters and uncertainty magnitudes that were used in the uncertainty analysis model to generate the GIFTS calibration accuracies. Even including the uncertainty due to the characterization of the telescope transmission in-flight, the expected calibration accuracy is well within the nominal 1 K requirement for accurate atmospheric sounding. The estimates shown in Figures 1 and 2 are derived from specifications presented at the GIFTS preliminary design review and will be updated following the critical design review. The optimal methodology for the determination of telescope transmission on-orbit continues to be a subject of ongoing research.

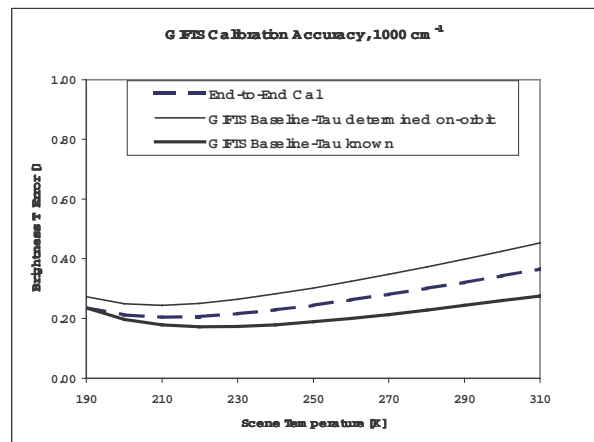


Figure 1. Calibration uncertainty estimate at  $1000 \text{ cm}^{-1}$  comparing a large aperture external "End-to-End" calibration target to the GIFTS baseline design which uses two high emissivity targets located behind the telescope. Tau is the telescope transmission.

Table 1. Calibration uncertainty analysis

Input Parameters		
wn	Wavenumber	See figures.
tau	Telescope (2) elements and blackbody mirror transmission	0.913
Thbb	Hot blackbody temperature	300 K
Tcbb	Cold blackbody temperature	265 K
Tspace	Temperature of space	4 K
Ttel	Telescope temperature	265 K
Tstr	Temperature of structure reflecting into BB's	265
Ehbb	Emissivity of hot blackbody	0.996
Ecbb	Emissivity of cold blackbody	0.996
Parameters Used For Temperature Stability		
Etel	Telescope emissivity	0.087
TauTot	Total transmission through instrument	0.205
TtelΔ	Change in telescope temp between earth and space views	0.5 K
Uncertainty Magnitudes		
ΔThbb	0.07 K	
ΔTcbb	0.07 K	
ΔEhbb	0.002 K	
ΔEcbb	0.002 K	
ΔTstr	5 K	
Δtau	0.0086 RSS	
ΔTtel	2 K	

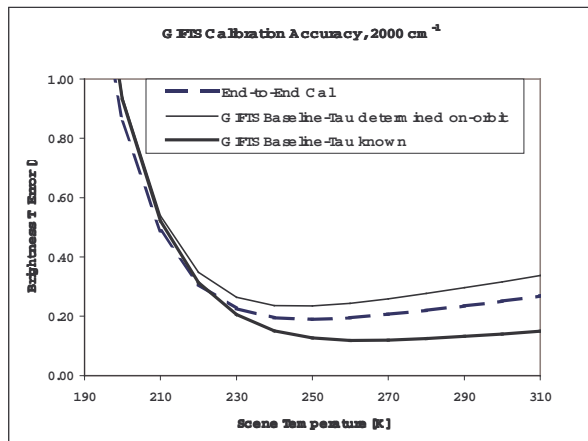


Figure 2. Same as Figure 1 but at 5 microns.

### 3.4 Spectral Calibration

The spectral calibration used for GIFTS will build upon the experience of ground-based and aircraft FTS systems (AERI, HIS, S-HIS, and NAST-I) designed with a single on-axis field-of-view (FOV) (Revercomb et al. 1998, Cousins and Smith 1997). The spectral characteristics of these instruments can be defined by an Instrument Line Shape (ILS) and a spectral sampling interval. The observed spectrum is the atmospheric spectrum convolved with the ILS and sampled at equally spaced points starting at zero wavenumber.

The spectral sampling scale is maintained very accurately by the stable laser used to trigger sampling at equal intervals of Optical Path Difference (OPD). Because the wavenumber samples are known to be equally spaced as well, the calibration of this spectral scale is determined for an entire, broad spectral band by the determination of the proper wavenumber for any single spectral feature in the band. We use the comparison of observed atmospheric spectra to line-by-line radiative transfer calculations (based on observed atmospheric state parameters) to determine the proper wavenumber scale. This calibration process transfers the very accurate positions of prominent spectral line features in the HITRAN database to the observed spectral scale (Rothman et al. 1998). An effective laser wavenumber parameter is used to describe this scale.

An example of the spectral scale calibration process is shown for observations of upwelling infrared radiance from the UW S-HIS aircraft instrument during the NASA KWAJEX experiment. Figure 4 shows a comparison of measured and calculated S-HIS spectra for the 722–738 cm<sup>-1</sup> spectral region from a clear sky flight of the NASA DC-8 aircraft on 12 September 1999. This spectral region has been chosen for spectral calibration, because of the high accuracy of the measured spectral line parameters of the dominant CO<sub>2</sub> absorption lines in this region. Figure 4 shows integrated residuals (observed minus calculated) for this spectral region versus the unit-less quantity of the effective laser wavenumber divided a reference wavenumber value. There is a well defined minimum in this curve, which can be used to determine the S-HIS spectral calibration. From an analysis of many similar cases collected over the DOE ARM site in north central Oklahoma (Tobin et al. 2003), the S-HIS effective laser wavenumber (and spectral calibration) has been determined with an accuracy of ~1 part in a million. Similar accuracy is expected for the GIFTS spectral calibration.

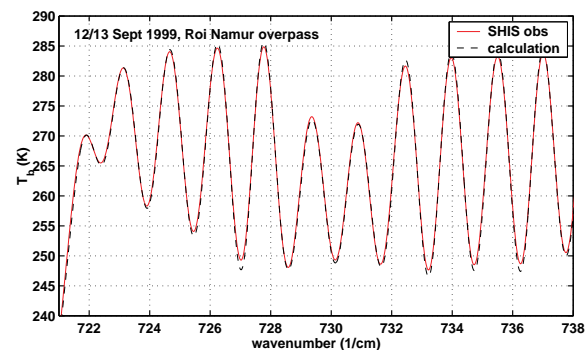


Figure 3. Observations of the regularly spaced CO<sub>2</sub> emission lines in the upwelling infrared radiance obtained by the UW Scanning HIS instrument are compared to a line-by-line calculation based upon a coincident radiosonde temperature and water vapor vertical profile and the HITRAN spectroscopic database.



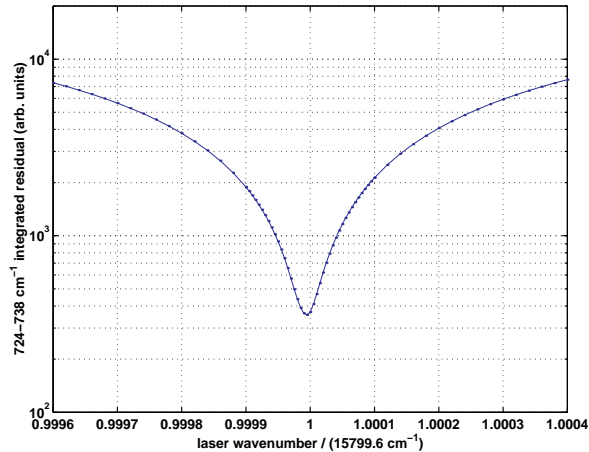


Figure 4. Fitting the residuals (observed-calculated) in the 724 to 738  $\text{cm}^{-1}$  region for the effective S-HIS laser wavenumber by adjusting the observed wavenumber scale in the range of -0.04% to +0.04%.

The major difference between GIFTS and these single-FOV instruments is that each pixel of its imaging detector array has a different wavenumber scale. This effect is a very predictable result of the different angles traversed through the interferometer by the beams focused on each pixel. While the central pixel is nominally the same as the single FOV instruments discussed above, off-axis detectors are irradiated by beams passing through the interferometer at non-zero mean angles. A non-zero mean angle causes the OPD for any given position of the interferometer Michelson mirror to be reduced by the cosine of the off-axis angle. This OPD scale variation with pixel location is illustrated in Figure 5, which shows a simulated interferogram for the GIFTS longwave band with a uniform scene. For the longwave FPA, the double sided interferogram is sampled at 2048 points. The exact OPD sampling positions, however, vary for each pixel depending on the mean off-axis angle, and the single pixel half-angle,  $b$ . The magnified portion of the interferogram illustrated in Figure 5 shows the 0.66 cm region enhanced by the equal spacing of 15 m CO<sub>2</sub> lines. Three individual OPD points from an on-axis interferogram (0.6637, 0.6654, 0.6671 cm) are also shown for every pixel along the diagonal from the center to a corner pixel of the detector array. Note that all of the points fall on the same continuous interferogram. For this uniform scene, the only significant difference is a small change in the OPD sampling interval. In other words, the differences can be rigorously eliminated by interpolation to a standard reference wavenumber scale.

The on-orbit spectral calibration process for GIFTS will make use of comparisons of observations with detailed radiative transfer calculations in order to assign a wavenumber scale to each field of view in each of the two GIFTS focal plane arrays. The plan for resampling of the GIFTS spectra to a common wavenumber grid is described in a subsequent section.

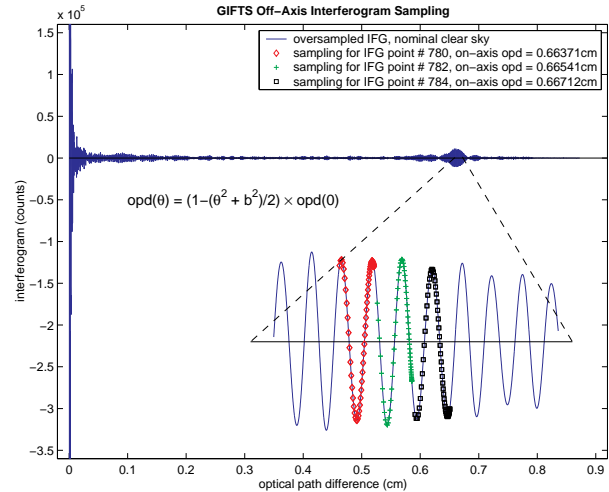


Figure 5. Illustration of the OPD sampling variations due to off-axis beams. The off-axis pixels sample the interferogram at smaller OPDs (compared to the on-axis beams), according to the given equation for  $\text{OPD}(\theta)$ . For three different on-axis sample points, the range of off-axis sampling points (from the near-center pixels to the corner pixels of the focal plane array) are shown in the blowup.

### 3.5 Instrument Line Shape Correction

To first order, the ILS is a sinc function ( $\sin(x)/x$ ). However, for accurate radiometry, it is important to make sure that the FOV is carefully aligned about the central axis of the interferometer and that an effective  $b$  is determined. Again, we use comparisons with specific regions of calculated atmospheric spectra to refine our nominal values of  $b$  (based on optical design). The finite field-of-view effect on ILS for the AERI, Scanning HIS and NAST-I instruments is negligible for the longwave band, but can be significant in the shortwave band. Procedures to remove the relatively small effects of ILS are routinely applied to the data from AERI, Scanning HIS and NAST-I. A similar behavior is realized for the geostationary orbiting GIFTS because of the extremely small range of angles contributing to each individual detector pixel ( $<1$  mrad in the interferometer). As a result, the variation of ILS across the array is extremely small and could even be ignored without introducing significant errors. The ILS is essentially a pure sinc function and exhibits extremely small ILS differences between the on-axis and extreme-diagonal pixels. In the GIFTS primary sounding mode, the self-apodization is very small—less than 1% over the array. In fact, because of the very small angles involved for GIFTS, the deviations from a pure sinc-function ILS are significantly smaller than for the aircraft and ground-based instruments discussed above. Figure 6 shows that the peak brightness temperature effect of ignoring ILS variations is less than 0.15 K for a typical earth scene.

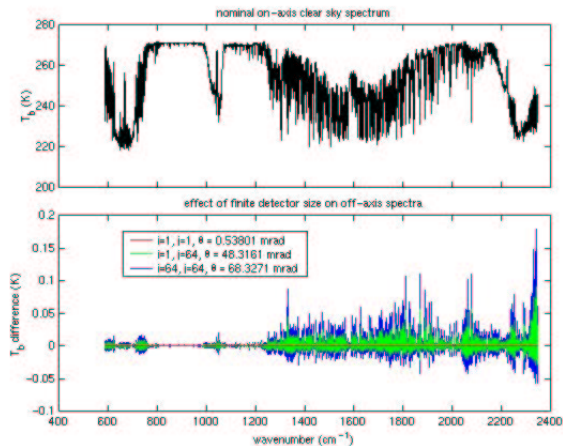


Figure 6. A nominal clear sky spectrum (top panel) and the magnitude of the finite detector size self-apodization effect in brightness temperature (bottom panel) for three FPA pixel locations. In the bottom panel, the  $i, j = (1,1)$  curve is the dark curve near zero, the  $i, j = (1,64)$  has a slightly larger magnitude, and the  $i, j = (64,64)$  curve has the largest magnitude.

### 3.6 Wavenumber Resampling (Off-axis Correction)

Once the spectral calibration is determined for each of the fields of view, the GIFTS radiance spectrum can be re-sampled from the original sampling interval to a standard reference wavenumber scale. The re-sampling can be performed in software using an FFT, "zero padding", and linear interpolation of an over-sampled spectrum. An alternative approach using a convolution rather than an FFT to resample the spectra will be evaluated for possible performance advantages. The result of the wavenumber resampling operation will be that all of the GIFTS spectra will have a common wavenumber scale independent of their location in the focal plane array. This is essential for the routine comparison of observations and radiative transfer calculations needed in the production of Level 2 products, e.g. temperature and humidity profiles.

### ACKNOWLEDGEMENTS

This work was recently supported by NOAA federal grant NAO7EC0676 with previous support under NASA contract NAS1-00072.

### REFERENCES

Best, F. A., H. E. Revercomb, G. E. Bingham, R. O. Knuteson, D. C. Tobin, D. D. LaPorte, and W. L. Smith, 2000: Calibration of the Geostationary Imaging Fourier Transform Spectrometer (GIFTS), presented at SPIE's Second International Asia-Pacific Symposium on Remote Sensing of the Atmosphere, Environment, and Space, Sendai, Japan, 9–12 October 2000.

Best, F., H. Revercomb, D. LaPorte, R. Knuteson, and W. Smith, 1997: Accurately calibrated airborne and ground-based Fourier Transform Spectrometers II: HIS and AERI calibration techniques, traceability, and testing, presented at the Council for Optical Radiation Measurements (CORM) 1997 Annual Meeting, National Institute of Standards and Technology (NIST), Gaithersburg, MD, April 29, 1997.

Bingham, G. E., R. J. Huppi, H. E. Revercomb, W. L. Smith, F. W. Harrison, 2000: A Geostationary Imaging Fourier Transform Spectrometer (GIFTS) for hyperspectral atmospheric remote sensing, presented at SPIE's Second International Asia-Pacific Symposium on Remote Sensing of the Atmosphere, Environment, and Space, Sendai, Japan, 9–12 October 2000.

Cousins, D., and W. L. Smith, 1997: National Polar-Orbiting Operational Environmental Satellite System (NPOESS) Airborne Sounder Testbed-Interferometer (NAST-I), *Proceedings of SPIE*, **3127**, 323-331.

Dittberner, G. J., James J. Gurka, and Roger W. Heymann, 2003: NOAA's GOES satellite program—status and plans, 19th Conference on IIPS, 83rd Annual Meeting, 8–13 February 2003, Long Beach, CA. Published by the American Meteorological Society, Boston, Mass.

Gurka, J. J., Gerald J. Dittberner, Pamela Taylor, and Timothy J. Schmit, 2003: Specifying the requirements for imaging and sounding capabilities on the GOES-R series, 12th Conference on Satellite Meteorology and Oceanography, 83rd Annual Meeting, 8-13 February 2003, Long Beach, CA. Published by the American Meteorological Society, Boston, Mass.

Huang, H-L., J. Li, E. Weisz, K. Baggett, J. E. Davies, J. R. Mecikalski, B. Huang, C. S. Velden, R. Dengel, S. A. Ackerman, E. R. Olson, R. O. Knuteson, D. Tobin, L. Moy, D. J. Posselt, H. E. Revercomb, and W. L. Smith, 2004: Infrared hyperspectral sounding modeling and processing, 20th Conference on IIPS, 84th AMS Annual Meeting, 11-15 January 2004, Seattle, WA. Published by the American Meteorological Society, Boston, Mass.

Limaye, S. S., T. Smith, R. O. Knuteson, H. E. Revercomb, 2004: Geolocation of the Geosynchronous Imaging Fourier Transform Spectrometer (GIFTS) data, 20th Conference on IIPS, 84th AMS Annual Meeting, 11-15 January 2004, Seattle, WA. Published by the American Meteorological Society, Boston, Mass.

Revercomb, H.E., V.P. Walden, D.C. Tobin, J. Anderson, F.A. Best, N.C. Ciganovich, R.G. Dedecker, T. Dirkx, S.C. Ellington, R.K. Garcia, R. Herbsleb, R.O. Knuteson, D. LaPorte, D. McRae, and M. Werner, 1998: Recent results from two new aircraft-based Fourier transform interferometers: The Scanning High-resolution Interferometer Sounder and the NPOESS

- Atmospheric Sounder Testbed Interferometer, 8th International Workshop on Atmospheric Science from Space using Fourier Transform Spectrometry (ASSFTS), Toulouse, France, 16-18 November 1998.
- Revercomb, H. E., F. A. Best, R. G. Dedecker, T. P. Dirkx, R. A. Herbsleb, R. O. Knuteson, J. F. Short, and W. L. Smith, 1993: Atmospheric Emitted Radiance Interferometer (AERI) for ARM. In Fourth Symposium on Global Change Studies, January 17–22, 1993, Anaheim, California. Published by the American Meteorological Society, Boston, Mass.
- Revercomb, H. E., H. Buijs, H. B. Howell, D.D. LaPorte, W. L. Smith, and L. A. Sromovsky, 1988: Radiometric calibration of IR Fourier Transform Spectrometers: solution to a problem with the High Resolution Interferometer Sounder", *Appl. Opt.*, **27**, 3210–3218.
- Rothman, L. S., et al., 1998: The HITRAN Molecular Spectroscopic Database and HAWKS: 1996 Edition, *Journal of Quantitative Spectroscopy and Radiative Transfer*, **60**, pp. 665-710.
- Smith, W. L., D. K. Zhou, F. W. Harrison, H. E. Revercomb, A. M. Larar, A. H. Huang, B. Huang, 2000: Hyperspectral remote sensing of atmospheric profiles from satellites and aircraft, presented at SPIE's Second International Asia-Pacific Symposium on Remote Sensing of the Atmosphere, Environment, and Space, Sendai, Japan, 9–12 October 2000.
- Tobin, D. C., H. E. Revercomb, R. O. Knuteson, 2003: On-orbit Spectral Calibration of the Geosynchronous Imaging Fourier Transform Spectrometer (GIFTS), in Proceedings of CALCON 2003, Characterization and Radiometric Calibration for Remote Sensing, Space Dynamics Laboratory / Utah State University, Logan, Utah, 15-18 September 2003.